Ferromagnetic nanoclusters in two-dimensional ^{3}He

E. Collin, C. Bäuerle, Yu. M. Bunkov, and H. Godfrin
Centre de Recherches sur les Très Basses Températures, Laboratoire Associé à l'Université J. Fourier et à l'Institut National Polytechnique de Grenoble, Centre National de la Recherche Scientifique, Boîte Postale 166, 38042 Grenoble Cedex 9, France
(Received 10 October 2005; published 23 March 2006)

^{3}He adsorbed on graphite is an almost ideal two-dimensional (2D) fermionic system. The 2D solid, where the interaction between the nuclear spins $S=\frac{1}{2}$ is due to multiple spin exchange, has been extensively studied as a model system for strongly interacting fermions in 2D. At high densities in the second layer, three-body exchange dominates and leads to Heisenberg ferromagnetism. We report on nuclear magnetic resonance measurements at ultralow temperatures and low magnetic fields of the second layer of ^{3}He on graphite preplated by one layer of ^{4}He. By adding controlled amounts of ^{4}He, ^{3}He atoms are pushed out from the ferromagnetic domains, which become smaller and denser. We can evaluate the properties of these clusters, and control their size from a few tens to a few hundreds of atoms. These sizes are comparable to today's computing capabilities for exact numerical calculations on small clusters, and should lead to direct comparison between measurements on this model Heisenberg system and theory.

DOI: 10.1103/PhysRevB.73.125421 PACS number(s): 75.70.Ak, 75.10.Jm

The Heisenberg Hamiltonian is of ubiquitous interest in condensed matter physics. It was first proposed by Heisenberg[1] in 1926 to account for the magnetic properties of solids. This Hamiltonian is a direct consequence of fermions exchange,[2] when only two-body and three-body exchange rings are allowed, the first favoring antiferromagnetism and the latter ferromagnetism.[3] The Heisenberg Hamiltonian is thus of fundamental nature, and even though it is quite difficult to solve, it is extraordinarily simpler than the original problem of interacting fermions. One of the peculiar properties of this Hamiltonian is that it does not generate a phase transition in dimensions smaller than 3.[4]

I. THE 2D-^{3}He SYSTEM

^{3}He atoms can be adsorbed on graphite to form two-dimensional (2D) $S=\frac{1}{2}$ nuclear magnetic systems. The large binding energy, of the order of 100 K, ensures that at mK temperatures the system is perfectly confined in a plane. The large size of exfoliated graphite platelets ($\approx$500 Å for Papyex[5] sheets) used as a substrate makes it suitable for 2D studies. The 2D solid is described by the multiple spin exchange model (MSE),[6,7] the exchange constants being a function of the area density.[8] At low densities, (cyclic) exchange processes up to six bodies are relevant, which leads to a strong quantum frustration, each process favoring a different symmetry. The ground state is a *spin liquid*,[9] realized in the commensurate second layer.[10–14] When this solid ^{3}He second layer densifies, three-body exchange finally dominates and the system becomes an almost perfect 2D Heisenberg ferromagnet[15–17] with exchange J in the mK range. The solid then forms a triangular Bravais lattice incommensurate with the underlying layer.

In this paper, we report on continuous wave nuclear magnetic resonance (cw-NMR) measurements performed on the ferromagnetic system down to about 100 μK. The first solid layer has been replaced by ^{4}He ($S=0$ and hence nonmagnetic), the binding energy of which is higher than for ^{3}He due to its larger mass. The key feature of the present experiment is that by adding controlled amounts of ^{4}He (and keeping the quantity N_{total} of ^{3}He constant, 2.97 ccSTP for an incommensurate sample surface area of 13.6 m^2), we can change the size and density of the ferromagnetic regions. We demonstrate our capability of confining small 2D clusters of ^{3}He atoms where the dominant interaction is ferromagnetic exchange.

A run at a submonolayer coverage ($N_{\text{submono}}=9.28$ at/nm^2), where the magnetic susceptibility follows a Curie law $C_N N_{\text{submono}}/T$ (C_N is the Curie constant per atom), enables us to calibrate the NMR-spectrometer and to verify that the cell is in good thermal contact with the thermometers in the entire temperature range (0.1–400 mK). The temperature is measured using a pulsed Pt-NMR thermometer and a calibrated carbon resistance thermometer. A low magnetic field (30.5 mT) is used in order to ensure that $\mu B \ll k_B T$ for all temperatures. For each introduction of gas in the cell, the sample is annealed at 4 K for at least a day, and then slowly cooled down. Further experimental details are given elsewhere.[18]

In a previous paper,[10] we have shown that for ^{4}He coverages between 6.56 ccSTP and 7.64 ccSTP, the so-called $\frac{4}{7}$ commensurate phase is stable; adding ^{4}He simply promotes ^{3}He atoms from the solid second layer to the fluid third layer. Both contributions are resolved by fitting the total magnetization to the sum of a solid term and a liquid term, above roughly 5 mK,

$$M = C_N\left(\frac{N_{\text{solid}}}{T-\theta} + \frac{N_{\text{liquid}}}{\sqrt{T^2+T_F^2}}\right) \tag{1}$$

with obviously $N_{\text{total}}=N_{\text{solid}}+N_{\text{liquid}}$. The expression for the solid magnetization is valid at high temperatures, θ being the Weiss temperature assigned to the solid contribution, i.e., for a single triangular Heisenberg magnet $\theta=3J$. The expression describing the magnetization of the liquid was first proposed by Dyugaev,[19] T_F being the Fermi temperature. The energy

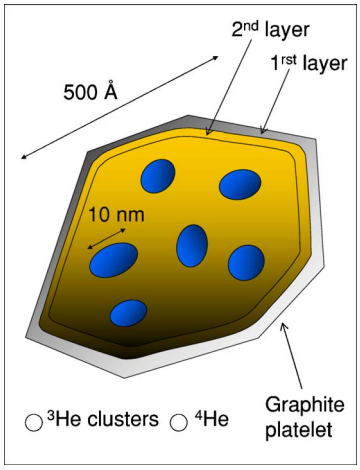

FIG. 1. (Color online) Schematic view of a graphite platelet covered by a ^{3}He–^{4}He solid mixture. Atoms are not represented. A 10 nm cluster contains about 500 ^{3}He atoms.

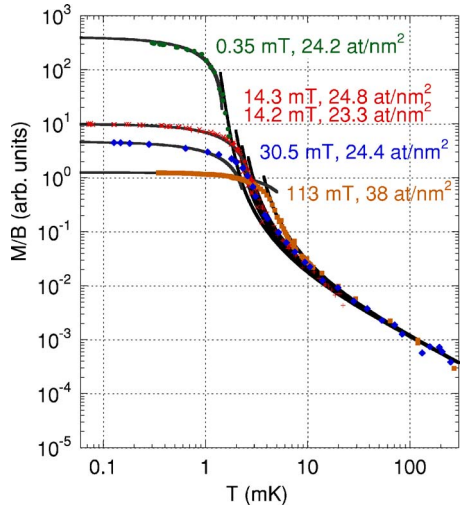

FIG. 2. (Color online) Comparison of different results on 2D ferromagnetic solid ^{3}He. From top to bottom: data from Bozler *et al.* (Ref. 28) (circles), from Godfrin *et al.* (Ref. 17) and Schiffer *et al.* (Ref. 21) (two types of crosses), this work (diamonds), and from Bäuerle *et al.* (Refs. 23 and 27) (squares). All data were normalized to the same quantity of spins. Details are given in the text.

scales are clearly separated, since $\theta \simeq 1$ mK and $T_F \simeq 300$ mK.

^{3}He atoms trapped at heterogeneities[20] that are known to give rise to a close-to-paramagnetic signal are first removed by the adjunction of ^{4}He at the beginning of the $\frac{4}{7}$ stability plateau. We do believe that these strong binding sites are responsible for the discrepancies in the experimental results[10,12] obtained at extremely low temperatures in the *spin liquid* regime. Finally, at a ^{4}He quantity of 8.04 ccSTP, which corresponds roughly to 40% ^{4}He atoms in the second layer, the system changes its nature: the sudden increase of the susceptibility below 5 mK indicates the onset of ferromagnetism.

In the next section, we describe experimental results on 2D ^{3}He–^{4}He mixture systems where the amounts of these isotopes are chosen in such a way that clusters of a few tens of atoms of ^{3}He are formed (Fig. 1). These nanoclusters display 2D Heisenberg ferromagnetic behavior, but in order to demonstrate this, some technical details about quasiparamagnetic strongly bound ^{3}He atoms must be discussed. Since these impurities affect all experiments on 2D ^{3}He, these results will be useful in a more general context. After this analysis, we obtain the magnetization of 2D Heisenberg nanoclusters as a function of size and temperature, which constitutes the main object of this paper.

II. FERROMAGNETIC ANOMALY

As for the pure ^{3}He case, this system passes through a "ferromagnetic anomaly"[16] when it densifies (that is, a density where J is maximum), ^{3}He atoms being also continuously promoted in the third fluid layer.[15,17,21–23] A comparison of the results obtained on ferromagnetic 2D solid ^{3}He is presented in Fig. 2.

2D ^{3}He ferromagnetism has been studied in various conditions, starting from the pure case[16] which displays a clear Heisenberg behavior, then replacing the first layer with a layer of ^{4}He (nonmagnetic),[24] or replacing it with HD,[25,26] giving rise to a low density ferromagnet frustrated by multiple spin exchange (not shown). ^{3}He on two layers of ^{4}He has been shown by Bäuerle *et al.*[23,27] to display a strong ferromagnetic tendency, proving thus the solidification of this weakly bound layer.

All but the data from Bäuerle *et al.* are obtained around the "ferromagnetic anomaly" (24 at/nm^2), in various magnetic fields from 0.35 to 113 mT. The cell substrate is Grafoil for Godfrin *et al.*[17] and Schiffer *et al.*, while for Bozler *et al.*[28] it is GTY Grade Grafoil. Experiments by Bozler *et al.*, Godfrin *et al.*, and Schiffer *et al.*[21] are performed on pure ^{3}He. For all these pure ^{3}He data, a paramagnetic contribution of order 28% of the atoms that are not located in the first layer has been subtracted. These atoms correspond to the strong binding sites already mentioned, and the proportion quoted here is consistent with values quoted in previous works.[17,21]

The lines are fits that will be explained in detail in the following. At high temperature, a series expansion of the Heisenberg model (with exchange parameter J) is used, defined as

$$\mathcal{H} = -2Jk_B \sum_{\langle i,j \rangle} \vec{S}_i \cdot \vec{S}_j, \tag{2}$$

while at low temperatures a spin wave calculation is taken (with cluster size N as a parameter): the full magnetization M_s of the ferromagnetic state present at $T=0$ is destroyed progressively by long wavelength bosonic excitations as one increases the temperature. Since the data are normalized to the same number of spins, the value of M_s/B in Fig. 2 is directly proportional to the inverse of the magnetic field B. The dependence on the magnetic field of the ferromagnetic magnetization has been experimentally demonstrated, for not too small fields, in Ref. 29, while keeping the density constant.

The experiment on the third-layer solid by Bäuerle *et al.*,[23,27] shown in Fig. 2, was carried out on the *same* Papyex cell as the present work, in a higher field. Both first and second layers were replaced by ^{4}He (11.344 ccSTP), and 7.943 ccSTP of ^{3}He were added to the system. From our NMR results (Fig. 7) and neutron diffraction data,[15] we can infer that for this experimental cell, 10.9 ccSTP fill the dense two first layers (respectively 11.6 at/nm^2 and 9.4 at/nm^2). Therefore, the ferromagnetic signal of Bäuerle *et al.*, which consists of only 30% of the ^{3}He atoms (the rest being fluid), comes solely from the third layer. For these data in Fig. 2, only the fluid contribution has been subtracted (before normalization). No strong binding site magnetization is seen, a fact that could be linked to the small ^{4}He quantity present in the third layer (about 0.45 ccSTP).

The exchange constants extracted from the high-temperature fits range from 1.6 to 2.1 mK for the second layer, and are explained by a dense (around 8 at/nm^2) incommensurate solid.[30] However, we fit the rather high value of 2.8 mK in the third solid layer, and estimate its density at about 6.2 at/nm^2, which is just above the fluid solidification.[31,32] The nature of this solid phase remains a puzzle, and one can simply conjecture that for such a low density, it should be commensurate with the underlying layer (a loose-packed $\frac{2}{3}$ phase[33]), a fact that could enhance the ferromagnetic exchange. Actually, this commensuration was already proposed by Greywall[34] in his attempt to describe the second-layer phase diagram in the ferromagnetic regime. More work is needed to understand the nature of this ferromagnetic exchange in the third layer. Indirect exchange through the overlying fluid layers may play a role in this solid very weakly bound to the substrate. Little is known on the multiple spin exchange coefficients in this layer, and it is also possible that higher-order contributions are significant (as in the second-layer HD preplated system[25,26]), although the Heisenberg fit is rather good.

The size of the ferromagnetic domains can be inferred through spin wave fits which lead to values ranging from 100 (our ^{4}He data) to 400 spins in Grafoil experiments, and 9000 for GTY Grade Grafoil. This illustrates the difference of platelet size in these substrates, the fits getting worse for fewer spins.

The following will focus on how the ^{3}He–^{4}He mixture studied in the present experiment crosses the "ferromagnetic anomaly" as one increases the density.

A. Before the anomaly

From 8.04 ccSTP to 9.15 ccSTP ^{4}He, the *spin liquid* commensurate phase slowly disappears while the proportion of ferromagnetic incommensurate phase grows. This could be performed by fractionizing the commensurate phase, or by slowly destroying it from its boundaries. Defects could be present (for instance vacancies, dislocations, walls), leading locally to density variations. Nevertheless, our analysis is consistent with a coexistence in the solid second layer of the commensurate *spin liquid* phase, and a denser *ferromagnetic* phase as proposed by Schiffer *et al.*[21] The actual microscopic structure remains unclear. However, at the coverage of 9.15 ccSTP where the commensurate phase has virtually totally disappeared, the NMR absorption line displays an unexpected shape at the lowest temperatures (Fig. 3, full line).

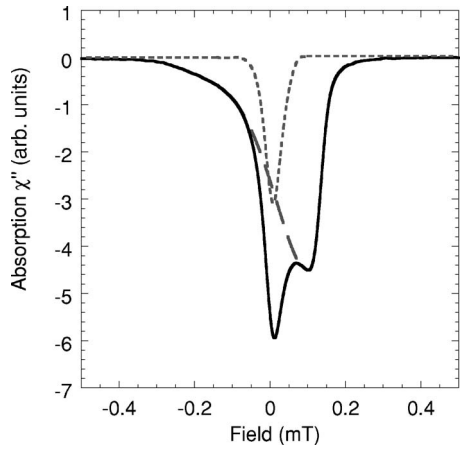

FIG. 3. NMR absorption signal measured at 150 μK with a ^{3}He coverage of 2.97 ccSTP and a ^{4}He coverage of 9.15 ccSTP (full line). No ^{3}He atoms are left in the first layer. The zero on the x axis is the Larmor field. The ferromagnetic contribution, long-dashed, and a close-to-paramagnetic contribution, short-dashed (see text), are resolved here.

B. At the anomaly

We clearly distinguish in the line structure two contributions. The first is a very broad one, asymmetric, which is characteristic of the ferromagnet, and is due to the dipolar field generated by the large polarization of the 2D solid (demagnetization effect).[17,21,35] The second one is very narrow, symmetric, and located in the spectrum at the Larmor frequency. This is the unambiguous signature of two different spin environments. It is possible to separate these contributions by empirically fitting a base line polynomial below the narrow peak (long-dashed line Fig. 3), and then subtracting the reconstructed ferromagnetic peak from the total line in order to get the narrow contribution (short-dashed line). We can use the same technique to separate all lines measured up to about 1 mK, where the two contributions cease to be resolved. Integrating each line separately gives the magnetization of each contribution, which is shown in Fig. 4 (low-temperature part, $T<2$ mK).

Since it is narrow and unshifted from the Larmor frequency, the narrow peak has to exhibit a low polarization. Within the error bars of the rough peak separation technique, we find a close-to-paramagnetic behavior for the narrow line contribution containing N_{para} spins (dashed line in Fig. 4). The inferred polarization of this solid is smaller than 15% for all temperatures. Subtracting from the total magnetization, at higher temperatures, the magnetic signal inferred from this fit, and the trivial liquid third-layer component, one obtains the ferromagnetic contribution in the whole temperature range (Fig. 4, $T>2$ mK), attributed to N_{ferro} spins verifying $N_{\mathrm{solid}}=N_{\mathrm{ferro}}+N_{\mathrm{para}}$.

Before pursuing the discussion, we shall comment on the reasons why this close-to-paramagnetic contribution has

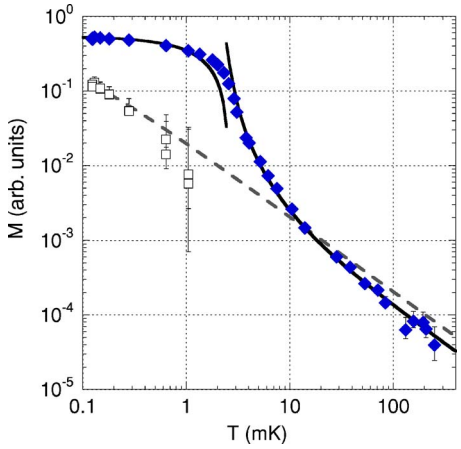

FIG. 4. (Color online) Magnetization as a function of temperature (^{4}He coverage 9.15 ccSTP). The full diamonds correspond to the main contribution, ferromagnetic. The squares come from the integration of the narrow contribution, displaying a close-to-paramagnetic behavior (see text). The lines are fits explained in the text. The error bars on the squares come from the empirical separation procedure (see text), the bars on the full diamonds come from the subtraction of the liquid contribution at high temperatures.

never been reported before. First of all, the first experiments were performed on *pure* ^{3}He samples.[17,21,35] In this case, a large peak at the Larmor frequency arising from the first layer masks any contribution in this region of the spectrum. Secondly, even in ^{4}He preplated samples, this contribution is difficult to see, and effectively we do resolve it only for the coverage of 9.15 ccSTP ^{4}He, because of the large difference in magnetization between the polarized ferromagnetic solid and the close-to-paramagnetic one. To resolve the latter, one has to have at least as many close-to-paramagnetic spins as ferromagnetic ones. In our case, we have about twice as many close-to-paramagnetic ^{3}He atoms as ferromagnetic ones.

The full lines in Fig. 4 are fits to the ferromagnetic data. At high temperature, we use a high temperature series expansion of the Heisenberg model (HTSE) valid for $N_{\text{ferro}} \to \infty$ and $J < T$,[36] and at low temperatures we use the spin wave expression derived by[17,37] (including the $k=0$ magnon, last term)

$$1 - \frac{M}{M_s} = \frac{T_0 + \frac{1}{S}T_m}{8\pi\sqrt{3}S^2 J}\left(1 - \frac{T}{T_0 + \frac{1}{S}T_m}\ln\left(e^{(T_0+(1/S)T_m)/T} - 1\right)\right) + \frac{1}{NS}\frac{1}{e^{(1/S)(T_m/T)} - 1} \tag{3}$$

with $T_m = \mu B / k_B$ the magnetic temperature, and $T_0 = 16\pi^2 SJ/N$ with N the effective size of the ferromagnetic domains. Note that N and N_{ferro} are not equal, as will become clear in the discussion below. The exchange constant extracted at high temperature $J \approx 2.05$ mK is consistent with published values (Figs. 2 and 6), although a little smaller. The difference could be attributed to size effects. Fixing J, we extract from the low-temperature fit the effective size of the ferromagnetic clusters $N \approx 120$ spins. We should point out that these two fits give *the same total number of ferromagnetic spins* through the low-temperature saturation magnetization M_s, and at high temperatures the ferromagnetic solid Curie constant $C_N N_{\text{ferro}}$ (via $M_s = C_N N_{\text{ferro}}/T_m$). This is the first time that such a consistency is reached, thus giving additional weight to the phase coexistence model in the second layer:[21] at the end of the completion of the second layer, the ferromagnet coexists with close-to-paramagnetic spins.

Then the question that arises is, where are these spins located? One conjecture would be to argue that these spins, about 20% of a layer, are trapped in *third-layer strong binding sites*. Effectively, these sites are known for the first and second layers,[10,20] and could also be present in the third layer

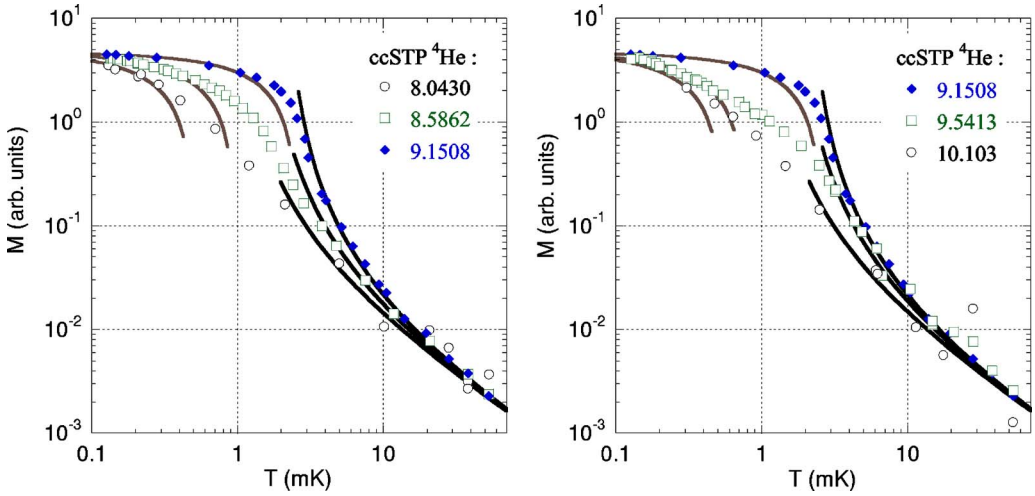

FIG. 5. (Color online) Evolution of the magnetization of nanoclusters of the ferromagnetic phase as one adds ^{4}He, as a function of temperature (before the ferromagnetic anomaly on the left, and after on the right). The fits are explained in the text. All curves have been normalized to the quantity of ferromagnetic spins. At high temperature, error bars (not shown) are due to the subtraction of the liquid component.

since it solidifies. The quality of the high- and low-temperature fits are discussed in the next section.

C. After the anomaly

As one continues to add ^{4}He, the second layer densifies and evolves toward a situation in which all ^{3}He atoms of the second layer are finally pushed in the third layer fluid. Although it is not possible to resolve a close-to-paramagnetic contribution, it is possible to see a signature of its presence by monitoring the position of the minimum of the NMR absorption line. As the weight of the magnetization passes from one spin ensemble to the other, as a function of temperature, one notices that the position of the line minimum shifts slightly from one frequency to another.[23] In contrast with the commensurate/incommensurate coexistence occurring before the anomaly, here the situation is simpler since both phases are incommensurate. Homogeneous compression of the ferromagnetic solid accompanied by the suppression of the localized spins is consistent with the data. From the phase coexistence model, we can then infer the number of ferromagnetic spins by measuring the saturation magnetization M_s. In the following, we will assume that the temperature dependence of the close-to-paramagnetic solid ^{3}He spins is the same as the one measured when both contributions were resolved (that is, close-to-paramagnetic). In Fig. 5, we present the magnetization as a function of temperature extracted for the ferromagnetic phase using this analysis. For simplicity, all the data are normalized to the quantity of ferromagnetic solid, and thus superimpose at low and high temperatures. The quantities of ^{4}He added are mentioned in the plot, and range from the beginning of the compression of the second layer to the end of the ^{3}He promotion to the third layer. Note that as one adds ^{4}He beyond 9.15 ccSTP, the quantity of close-to-paramagnetic spins also decreases. The lines are fits following the same procedure as described above, thus extracting an effective size for the ferromagnetic domains N, and an effective exchange constant J that could also be slightly size-dependent. Note that the high-temperature expression fits the data down to $(1.5-2)\times J$, and the low-temperature one up to $0.5\times J$. In between, the data smoothly interpolate between the two regimes. We believe that this interpolation law depends on the exact shape of the clusters, and is responsible for the fitting limits given above. Eventually with large N, low- and high-temperature fits practically join around 2 mK (Ref. 21) (see Fig. 2).

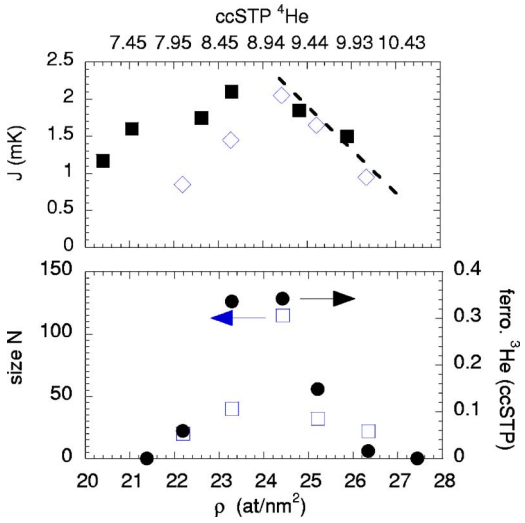

FIG. 6. (Color online) Parameters J (top, open diamonds) and N (bottom, open squares) extracted from the analysis, as a function of the total coverage. Values of J from Refs. 16 and 21, obtained in the pure ^{3}He system, are also displayed (full squares). The dashed line is a guide to the eye, emphasizing that the ferromagnetic phase progressively densifies, and vanishes. On the lower graph, the quantity of ^{3}He spins in the ferromagnetic phase N_{ferro} (full circles, right axis) is also displayed, in order to compare it to N (see text).

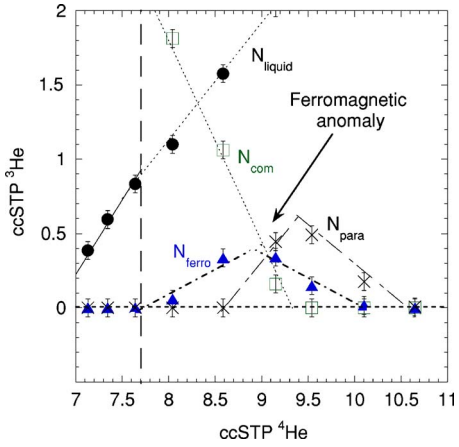

FIG. 7. (Color online) Quantity of ^{3}He spins attributed to the different phases in the present analysis N_{liquid}, N_{ferro}, N_{para}, and N_{com} (^{3}He atoms in the $\frac{4}{7}$ commensurate phase). Lines are guide to the eyes, and the vertical dashed line shows the beginning of the compression of the second layer.

III. DISCUSSION

The values for the parameters J and N are summarized in Fig. 6, together with the amount N_{ferro} of ferromagnetic solid ^{3}He in the second layer. These results can be directly compared with Ref. 21 (exchange data also displayed), since we clearly see the same "ferromagnetic anomaly," at a density for the total film that we compute to be roughly the same as that reported by these authors (about 24 at/nm). The exchange constants J are of the same order, but the effective sizes N are drastically *smaller* in our work (they quote 400 spins at the ferromagnetic anomaly, as fitted in Fig. 2). It should be noticed that in the present experiments, no sign of a finite temperature phase transition could be observed, in contrast with Ref. 38. An important experimental difference between our work and Ref. 38 lies in the strength of the magnetic field: although it is small compared to the exchange J, it remains large in our case in comparison with the dipolar field radiated by each spin, contrary to Ref. 38. Small anisotropies are simply washed out, and the dipolar term has been neglected in the spin wave calculation. Of course J and N cannot be regarded as accurate parameters. Indeed, we assumed the ferromagnetic islands to be simple-shaped, similar in size (line-tension arguments can be invoked to

justify these assumptions), and noninteracting with each other. We believe this is the source of the discrepancy between N, the effective size of the clusters, and the number of ferromagnetic spins in Fig. 6, a result pointed out also by Ref. 21. In our case, taking into account the incommensurate surface of the sample and the average platelet size, from N_{ferro} and N we estimate that about 15 clusters are present on each platelet. The possible presence of defects in the clusters has also not been addressed, and could be a suggestion for further theoretical and experimental work. In addition, the spin wave expression is certainly inaccurate for such a small number of spins, since we do not really reach the continuum limit needed for the $\vec{k}$ integration leading to Eq. (3). Nevertheless, the smallness of the ^{3}He clusters obtained in this work is certainly beyond doubt. As a comparison, the low-temperature fits of Fig. 2 give N about 400 and 9000 for Grafoil and GTY Grade Grafoil, respectively. A summary of the phase coexistence scenario developed here is given in Fig. 7.

In conclusion, we have measured using cw-NMR the magnetization of the second layer of ^{3}He adsorbed on graphite, using a ^{4}He preplating. By adding controlled amounts of ^{4}He, we could compress the commensurate system toward its ferromagnetic incommensurate state, and create ferromagnetic nanoclusters of adjustable average size. Although the parameters extracted cannot be taken as very accurate, the overall behavior is clearly established. The measured magnetization is amenable to direct comparison with theoretical calculations on small spin clusters governed by the Heisenberg Hamiltonian. These calculations would bring valuable information about the magnetization's actual dependence on boundary conditions.

[1] W. Heisenberg, Z. Phys. **38**, 441 (1926).
[2] P. A. M. Dirac, Proc. Phys. Soc. London **112A**, 661 (1926).
[3] D. J. Thouless, Proc. Phys. Soc. London **86**, 893 (1965).
[4] N. D. Mermin and H. Wagner, Phys. Rev. Lett. **17**, 1133 (1966).
[5] Papyex is a product of *Le Carbone Lorraine*.
[6] M. Roger, Phys. Rev. Lett. **64**, 297 (1990).
[7] M. Roger, C. Bäuerle, Yu. M. Bunkov, A.-S. Chen, and H. Godfrin, Phys. Rev. Lett. **80**, 1308 (1998).
[8] C. Bäuerle, Yu. M. Bunkov, A.-S. Chen, D. J. Cousins, H. Godfrin, M. Roger, and S. Triqueneaux, Physica B **280**, 95 (2000).
[9] G. Misguich, B. Bernu, C. Lhuillier, and C. Waldtmann, Phys. Rev. Lett. **81**, 1098 (1998).
[10] E. Collin, S. Triqueneaux, R. Harakaly, M. Roger, C. Bäuerle, Yu. M. Bunkov, and H. Godfrin, Phys. Rev. Lett. **86**, 2447 (2001).
[11] E. Collin, Yu. Bunkov, and H. Godfrin, J. Phys.: Condens. Matter **16**, S691 (2004).
[12] R. Masutomi, Y. Karaki, and H. Ishimoto, Phys. Rev. Lett. **92**, 025301 (2004).
[13] M. Siqueira, J. Nyéki, B. Cowan, and J. Saunders, Phys. Rev. Lett. **78**, 2600 (1997).
[14] K. Ishida, M. Morishita, K. Yawata, and Hiroshi Fukuyama, Phys. Rev. Lett. **79**, 3451 (1997).
[15] H. Godfrin and R. E. Rapp, Adv. Phys. **44**, 113 (1995).
[16] H. Franco, R. E. Rapp, and H. Godfrin, Phys. Rev. Lett. **57**, 1161 (1986).
[17] H. Godfrin, R. R. Ruel, and D. D. Osheroff, Phys. Rev. Lett. **60**, 305 (1988).
[18] C. Bäuerle, A.-S. Chen, Yu. M. Bunkov, H. Godfrin, and M. Roger, J. Low Temp. Phys. **113**, 287 (1998).
[19] A. M. Dyugaev, Sov. Sci. Rev., Sect. A **14**, 1 (1990).
[20] P. Schiffer, M. T. O'Keefe, D. D. Osheroff, and H. Fukuyama, Phys. Rev. Lett. **71**, 1403 (1993).
[21] P. Schiffer, M. T. O'Keefe, D. D. Osheroff, and H. Fukuyama, J. Low Temp. Phys. **94**, 489 (1994).
[22] P. Schiffer, M. T. O'Keefe, D. D. Osheroff, and H. Fukuyama, Phys. Rev. Lett. **71**, 1403 (1993).
[23] E. Collin, thèse de Doctorat, Université Joseph Fourier, Grenoble (2002).
[24] C. P. Lusher, J. Saunders, and B. P. Cowan, Europhys. Lett. **14**, 809 (1991).
[25] A. Casey, H. Patel, J. Nyéki, B. P. Cowan, and J. Saunders, J. Low Temp. Phys. **113**, 265 (1998).
[26] A. Casey, H. Patel, M. Siquiera, C. P. Lusher, J. Nyéki, B. P. Cowan, and J. Saunders, Physica B **284–288**, 224 (1999).
[27] C. Bäuerle, thèse de Doctorat, Université Joseph Fourier, Grenoble (1996).
[28] H. M. Bozler, Yuan Gu, Jinshan Zhang, K. S. White, and C. M. Gould, Phys. Rev. Lett. **88**, 065302 (2002).
[29] C. Bäuerle, Yu. M. Bunkov, S. N. Fisher, and H. Godfrin, Czech. J. Phys. **46**, Suppl. 1, 403 (1996).
[30] C. Bäuerle, Yu. M. Bunkov, A. S. Chen, D. J. Cousins, H. Godfrin, M. Roger, and S. Triqueneaux, Physica B **280**, 95 (2000).
[31] K.-D. Morhard, C. Bauerle, J. Bossy, Yu. Bunkov, S. N. Fisher, and H. Godfrin, Phys. Rev. B **53**, 2658 (1996).
[32] Note that the density of the commensurate $\frac{4}{7}$ phase in the second layer is 6.3 at/nm^2.
[33] M. Roger, C. Bäuerle, H. Godfrin, L. Pricoupenko, and J. Treiner, J. Low Temp. Phys. **112**, 451 (1998).
[34] D. S. Greywall, Phys. Rev. B **41**, 1842 (1990).
[35] H. M. Bozler, D. M. Bates, and A. L. Thomson, Phys. Rev. B **27**, 6992 (1983).
[36] J. Oitmaa and E. Bornilla, Phys. Rev. B **53**, 14228 (1996).
[37] P. Kopietz, P. Scharf, M. S. Skaf, and S. Chakravarty, Europhys. Lett. **9**, 465 (1989).
[38] L. J. Friedman, A. L. Thomson, C. M. Gould, H. M. Bozler, P. B. Weichman, and M. C. Cross, Phys. Rev. Lett. **62**, 1635 (1989).